ELSEVIER

February 1995

Materials Letters 22 (1995) 155–161

MATERIALS LETTERS

Observation of amorphous areas in a heavily cold rolled Cu–20 wt% Nb composite

D. Raabe *, U. Hangen

Institut für Metallkunde und Metallphysik, RWTH Aachen, Kopernikusstrasse 14, 52056 Aachen, Germany

Received 1 September 1994; accepted 17 November 1994

Abstract

A Cu-based metal matrix composite containing 20 wt% Nb was cast and heavily deformed by large strain cold rolling. During deformation, the initial Nb dendrites form into elongated filaments. The substructure of single Nb fibers was investigated by use of TEM, EDX and SAD. In heavily rolled specimens ($\epsilon = 99.4\%$), elongated dislocation cells as well as randomly arranged dislocations were observed. Furthermore, numerous amorphous areas were discovered within the Nb. Some of these non-crystalline areas extended over the entire filament width. The shrinkage of amorphous zones during heating was directly observed in the TEM.

1. Introduction

Cu and Nb have negligible mutual solubility in the solid state [1,2]. Fibre reinforced metal matrix composites (MMCs) consisting of a Cu matrix and 5–20 wt% Nb can hence be manufactured. Since the formation of elongated Nb filaments is simply achieved by heavy cold rolling [3–5] or wire drawing [6–11] of a cast ingot, the production technique employed is often referred to as in situ processing. Cu–Nb MMCs are well known for their very high strength and good electrical conductivity [3–11]. As was first demonstrated by Bevk et al. [6] and studied in detail by Spitzig an co-workers [3,7,8], tensile strengths exceeding 2000 MPa can be obtained after heavy wire drawing. Owing to its remarkable properties, MMCs consisting of Cu and Nb have been under thorough investigation in the past 15 years.

The current investigation is mainly concerned with the high strength of the composite. More precisely, the dominant goal of the study submitted is the examination of the microstructure of the Nb filaments extracted from a cold rolled Cu–20 wt% Nb MMC rather than measuring their average spacing and diameter. Whereas the examination of the topological features and electrical properties of Cu–20 wt% Nb has been subject to thorough investigations in the past (e.g. Refs. [3–11]), a detailed study tackling the microstructure of the Nb filaments, the isolation and preparation of which is highly intricate, was not yet submitted. In the work of Trybus and Spitzig on rolled Cu–20 wt% Nb [3] as well as in the analysis of Pelton et al. [12] on wire drawn samples, dislocation densities on the order of 10^{14} m^{-2} as well as areas completely void of dislocations were reported to occur in the Nb filaments. The discovery of their local amorphization, however, which is claimed to be the most relevant result of the present work, has not yet been discussed. The nomenclature in the field of metallic glasses is quite vague. The terms ''amorphous'' or ''non-crystalline'' commonly indicate the complete absence of structural regularity. The

* Corresponding author.

0167-577x/95/$09.50 © 1995 Elsevier Science B.V. All rights reserved
SSDI 0167-577x(94)00248-7

term "glassy" [13] accommodates the possibility of short or intermediate range order. However, since in the present case the exact state of order is not known, in the following the various terms are employed synonymously.

2. Experimental

2.1. Metallurgical processing, rolling deformation and annealing treatments

The Cu–20 wt% Nb alloy was melted in an induction furnace using a frequency of 10 kHz and a power of 30 kW [14–16]. Both constituents had a purity of about 99.99 wt%. Following the Cu–Nb phase diagram [1], a melting temperature of at least 1750°C is recommended for Cu 20 wt% Nb. Since other authors [2] reported the occurrence of a miscibility gap in the liquid phase owing to the presence of interstitial atoms like H, N, C and O, however, a temperature of 1830–1850°C was employed. Cu and Nb have similar densities ($\rho_{Cu} = 8890\ kg/m^3$, $\rho_{Nb} = 8580\ kg/m^3$). Gravitational segregation does hence not occur. Details concerning the metallurgical procedure are discussed elsewhere [4,14]. After casting, specimens were produced by cold rolling. The investigations were concentrated on filaments extracted from the three maximum rolling degrees achieved, namely $\epsilon = 97.2\%$, $\epsilon = 98.8\%$ and $\epsilon = 99.4\%$.

After having discovered non-crystalline areas in the Nb filaments, various annealing treatments were carried out in the TEM in order to directly observe crystallization. After a heat treatment at 573 K (30 min) and a subsequent annealing at 673 K (10 min) no crystallization was detected. During heating at 773 and 873 K, respectively ($t_{max} = 15$ min), the growth of crystalline into glassy areas was directly observed. After annealing at 873 K (15 min), the samples were cooled down to 673 K because crystallization proceeded too quick. The same applied for heat treatments at 923 K ($t_{max} = 10$ min) and 973 K ($t_{max} = 30$ min). The latter annealing led to complete crystallization of glassy areas.

2.2. Electron microscopy

For investigation of the Nb filaments, transmission electron microscopy (TEM) and for examining their morphology and topology scanning electron microscopy (SEM) was used. In order to avoid heating and mechanical loading of the specimens a new foil preparation technique was introduced. For providing flat sections, rolled samples were first cleaned in alcohol using ultrasonic vibrations. Subsequently, a thin Cu layer of some microns was removed by etching with a solution of 50 ml H_3PO_4 and 50 ml H_2O ($T = 268$ K, $U = 20$ V). In contrast to HNO_3 which also etches Nb, this solution exclusively affects the Cu matrix. After etching, the procedure was interrupted and the sample was cleaned again. In order to dissolute the Nb filaments laid open, in the subsequent step the specimen was etched in a solution of 50 ml alcohol, 50 ml HF and 20–30 ml HNO_3 ($T = 300$ K, $U = 0$ V). This successive procedure was repeated until perforation was nearly achieved. The last etching was then carried out by carefully dissolving the residual Cu close to the hole. By application of this technique any heating of the samples as is usually caused by mechanical thinning, dimpling (up to 450 K) or ion beam treatment (up to 600 K) was avoided.

The samples were examined employing a JEOL FX2000 operated at 200 kV using bright-field (BF), dark-field (DF) and selected area electron diffraction (SAD) techniques. For directly observing the structural regularity, high resolution transmission electron microscopy (HRTEM) was applied [17]. For this purpose a JEOL EX2000 operated at 200 kV was used. The chemical analysis was locally determined by use of energy-disperse X-ray spectrometry (EDX).

3. Results and evaluation

3.1. Morphology and dislocation arrangements

The as-cast Cu–20 wt% Nb sample contained primary Nb dendrites embedded in the Cu matrix. After dissolving the Cu using HNO_3, metallography was executed on isolated Nb dendrites (Fig. 1). The average diameter of the secondary dendrites was $d_0 = 2.2 \pm 0.4$ μm. After the highest deformation investigated ($\epsilon = 99.4\%$) an average filament thickness of 104 nm and minimum values of less than 50 nm were found. The average filament width after $\epsilon = 99.4\%$ was about 4000 nm (Fig. 2).

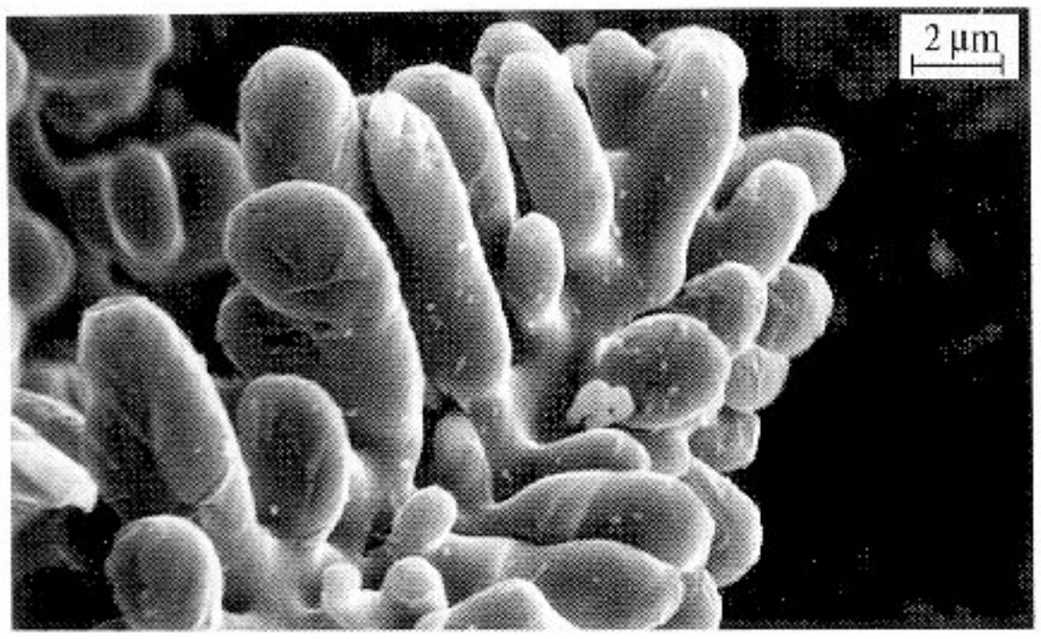

Fig. 1. Nb dendrite (as cast), chemically isolated from the Cu matrix (SEM).

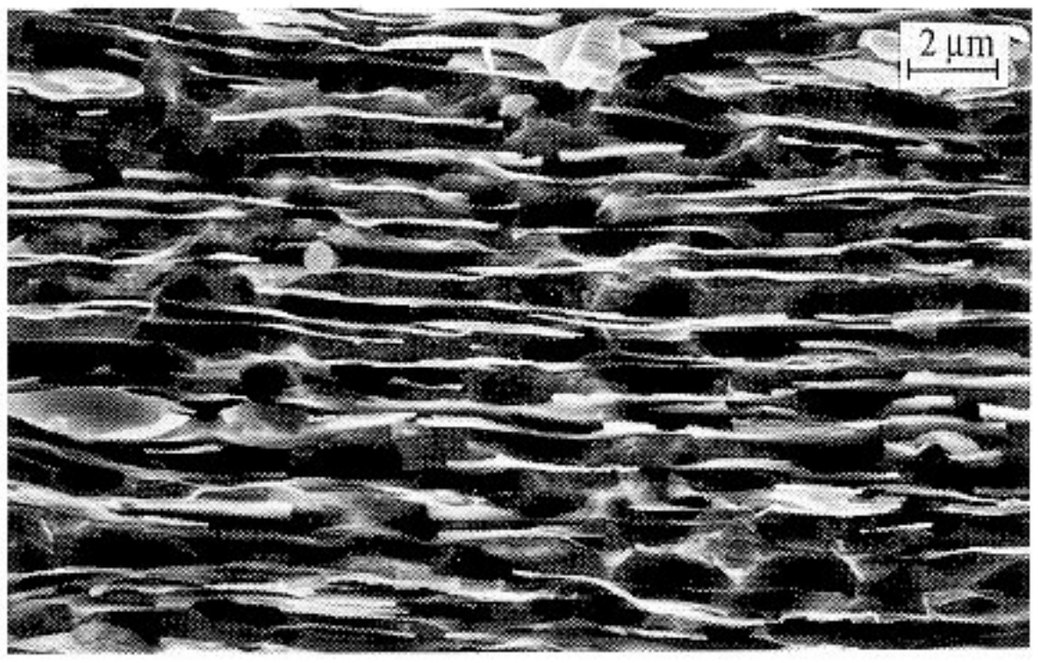

Fig. 2. Cu–20 wt% Nb composite, transverse section ($\epsilon = 99.4\%$).

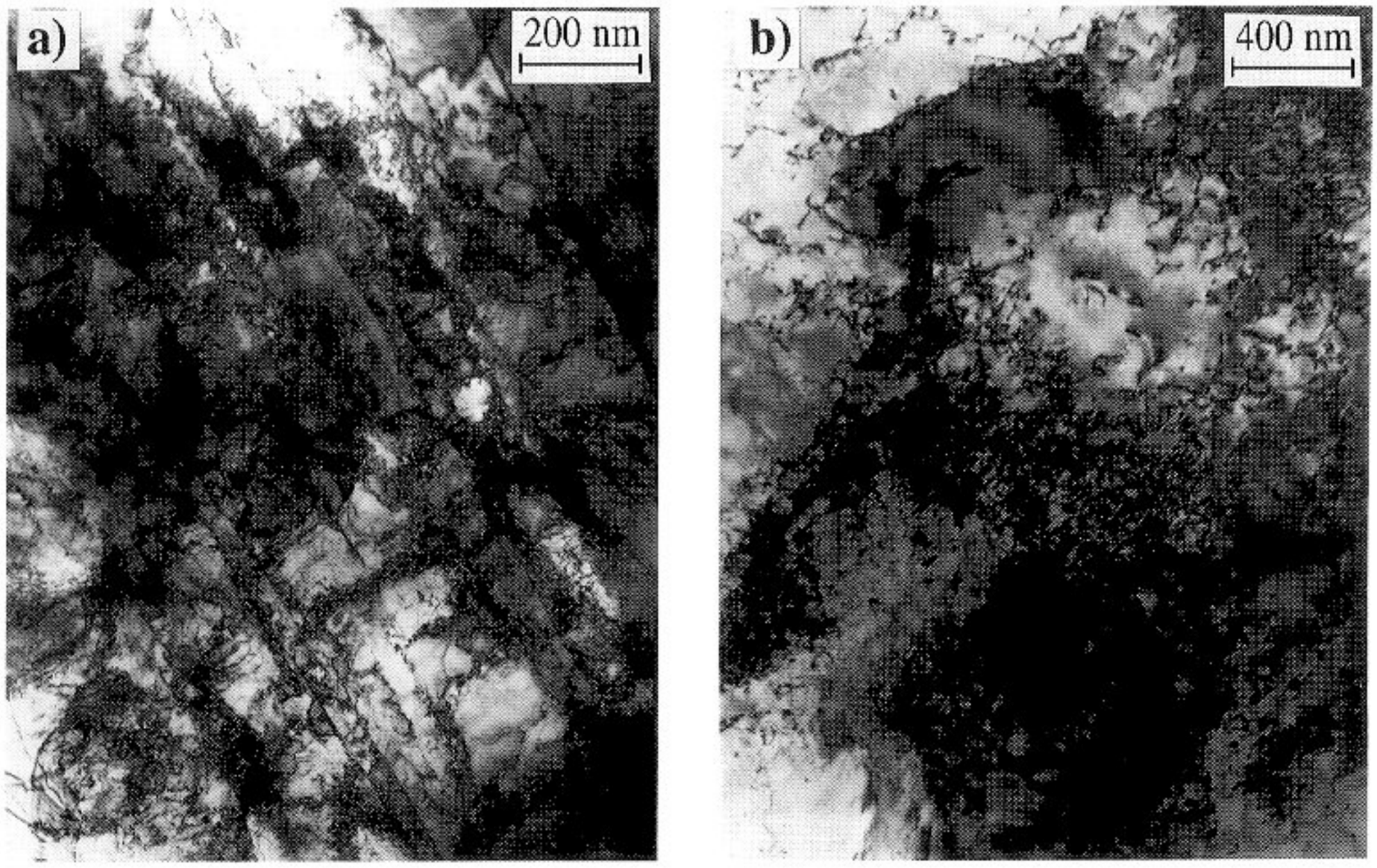

Fig. 3. Flat section of Nb filaments, TEM ($\epsilon = 99.4\%$). (a) Elongated dislocation cells. (b) Randomly arranged dislocations and dislocation tangles.

As is evident from Fig. 3 in filaments of all three deformation degrees investigated, elongated dislocation cells as well as densely arranged dislocation tangles were observed. Maximum dislocation densities of 10^{16} m^{-2} were determined locally in highly tangled areas (Fig. 3b). Furthermore, some areas containing only few elongated dislocations with densities, not exceeding 10^{12} m^{-2} were discovered.

3.2. *Non-crystalline areas in the Nb filaments*

In many Nb filaments which were extracted from cold rolled samples glassy areas were discovered. These regions frequently expanded over the entire filament width. In order to differentiate between the glassy state and simply dislocation free but crystalline areas (the occurrence of which was reported by Trybus and Spitzig [3]) the loss of structural regularity was in all cases checked by use of SAD, DF and HRTEM

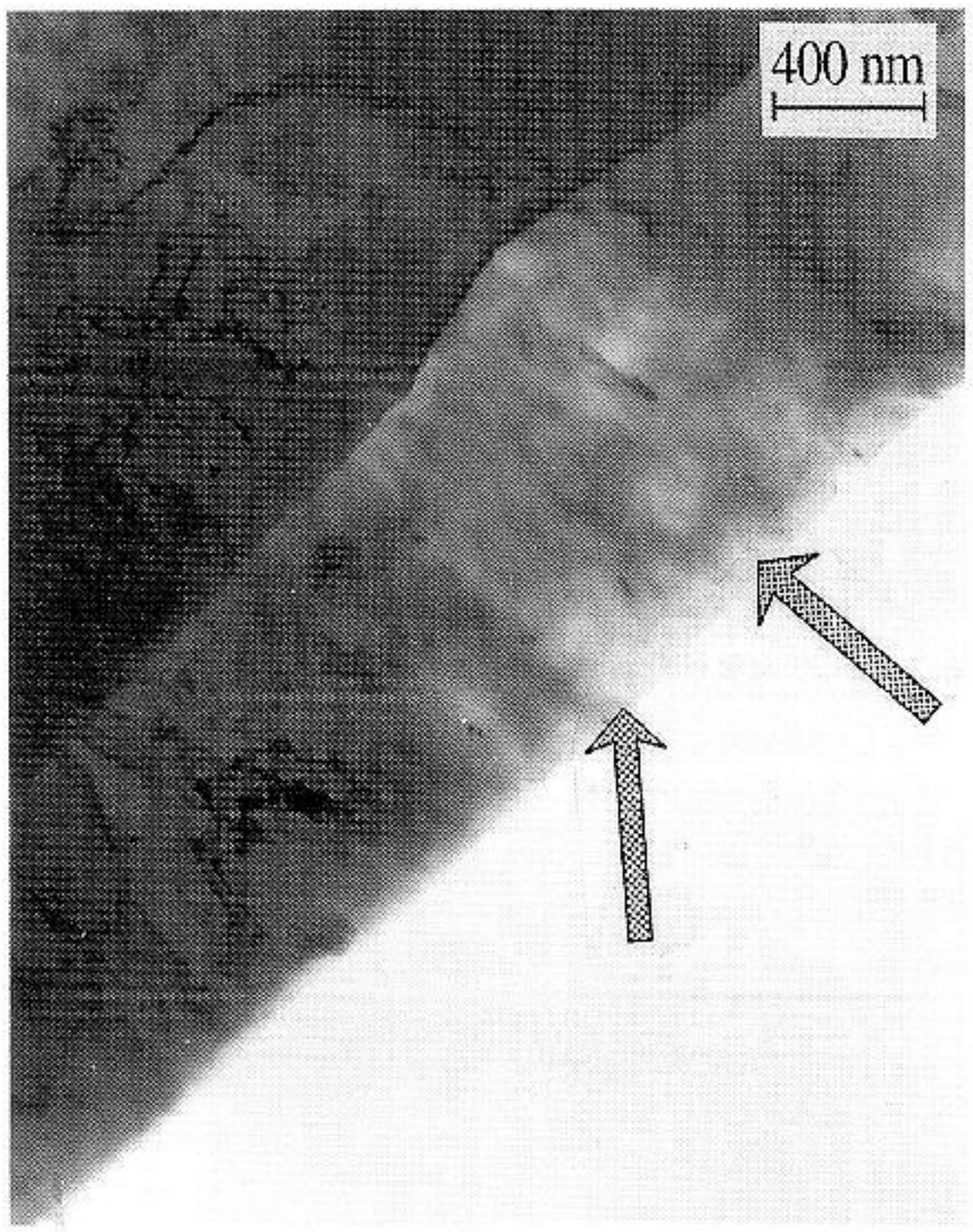

Fig. 4. Flat section of a Nb filament containing a glassy area (arrows) which extends over the entire filament width ($\epsilon = 99.4\%$).

[17]. By employment of EDX in the non-crystalline as well as in the neighboring crystalline areas an enhanced Cu content of up to 3.5 wt% was detected.

In Fig. 4 (arrow) a glassy area which is embedded within the crystalline matrix and extends over the entire width of the filament can be seen ($\epsilon = 99.4\%$). As is evident from Fig. 5 the SAD patterns supply evidence for the loss of structural regularity in the middle and the preservation of crystalline structure in neighboring areas. Whereas the pattern taken from the middle region clearly reveals the diffuse diffraction circles which are typically generated by amorphous materials, both adjacent regions show not only crystalline diffraction patterns but additionally similar orientations. An important feature of the micrographs taken from the non-crystalline areas is the absence of the lines stemming from the thickness contrast. By employing HRTEM [17] it was shown that the strict structural regularity of the atoms is partially destroyed and partially maintained, i.e. the structure observed is assumed to be not entirely amorphous.

In a filament of maximum deformation the process of crystallization during annealing was directly observed in the TEM. Whereas at temperatures below 773 K no distinct changes were observed, at 773 K already a slight shift of some phase boundaries separating crystalline from glassy areas was detected. During heat treatment at 873 K a considerable growth of some crystalline areas, leading to the shrinkage of the glassy region was detected. An area, where considerable movements of the phase boundaries were identified, is indicated by an arrow in Fig. 6 ($T = 873$ K, $t \approx 60$ s).

From the micrograph and the corresponding SAD patterns (Fig. 7) it is evident that the crystalline area, which was in smaller magnification shown in Fig. 6 (arrow) grows into the neighboring glassy region ($T = 873$ K, $t \approx 120$ s). After a subsequent heat treatment of 973 K ($t \approx 120$ s), followed by a quenching to 923 K, the initially amorphous filament area appeared partially crystallized (Fig. 8).

From the few micrographs and SAD patterns depicted here which were selected from a large number of comparable data it becomes evident that during heavy cold rolling in the Nb filaments of a Cu–20 wt% Nb composite massive phase transformation into the glassy state takes place.

3.3. Influence of non-crystalline regions on the strength

The influence of the presence of non-crystalline areas on the strength of the Nb filaments, which considerably affects the strength of the bulk sample, can be assessed by using standard dispersion hardening theory. More precisely, one has to estimate how the amorphous phase obstructs the movement of dislocations. It is presumed that the glassy areas are impenetrable to dislocations. Based on the observations presented (Figs. 6, 8) it is furthermore assumed that the glassy areas nucleate at the filament border rather than inside. This assumption implies that the Orowan mechanism is not relevant in the current case. The effective decrease of the filament width, however, gives rise to the increase of the critical stress required to activate the weakest dislocation source that can act between two interfaces [18],

$$\tau = \frac{A G_{\mathrm{Nb}} b_{\mathrm{Nb}}}{2\pi(1-\nu_{\mathrm{Nb}})t} \ln\left(\frac{t}{2b_{\mathrm{Nb}}}\right); \quad A \equiv 1.2,$$

where G is the shear modulus, b the Burgers vector, ν Poisson's ratio and t the filament width. If the effective,

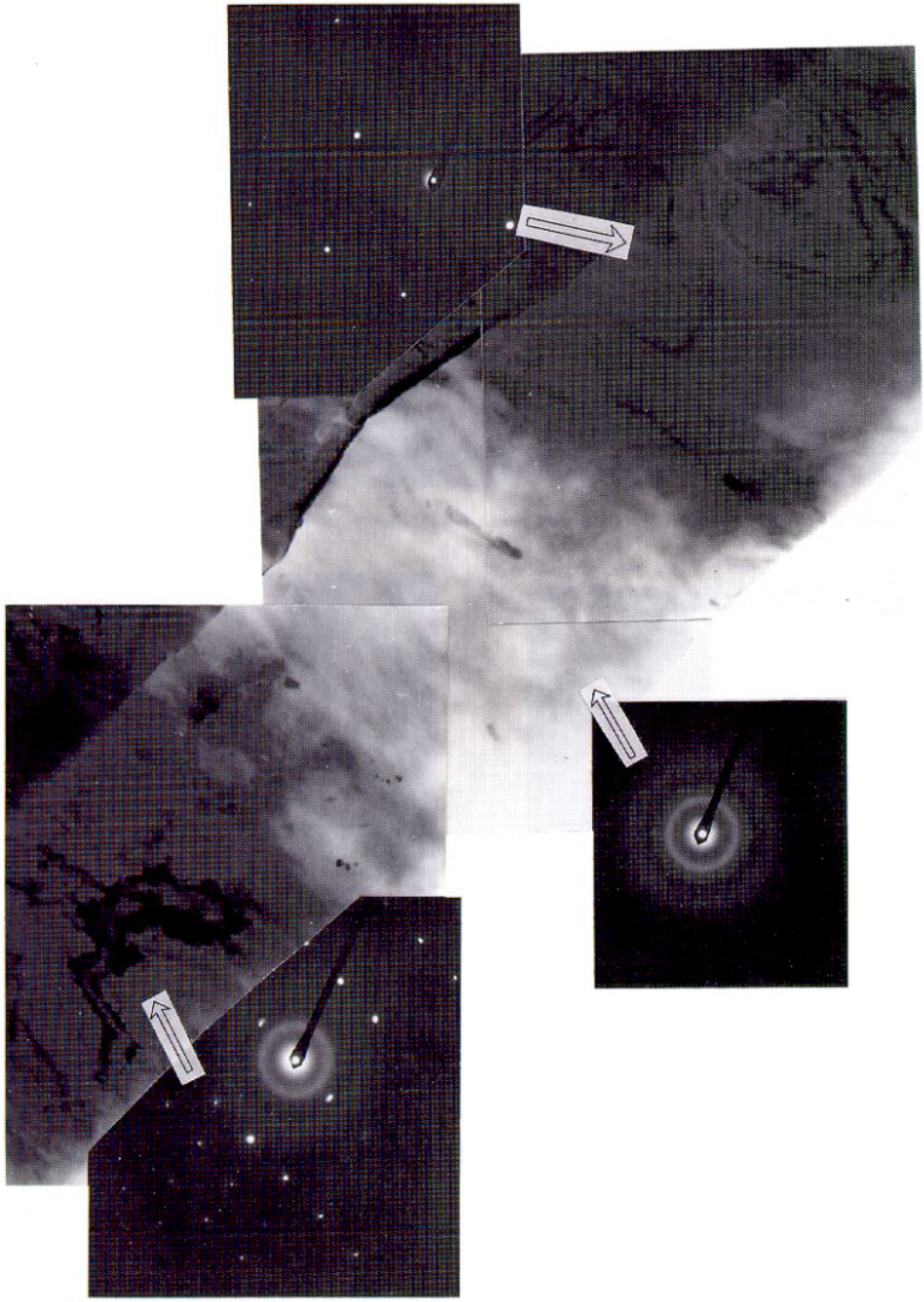

Fig. 5. Flat section of a Nb filament. Magnification of the scene shown in Fig. 4 ($\epsilon = 99.4\%$). SAD patterns suggest non-crystalline structure in the middle and crystalline structure in adjacent areas.

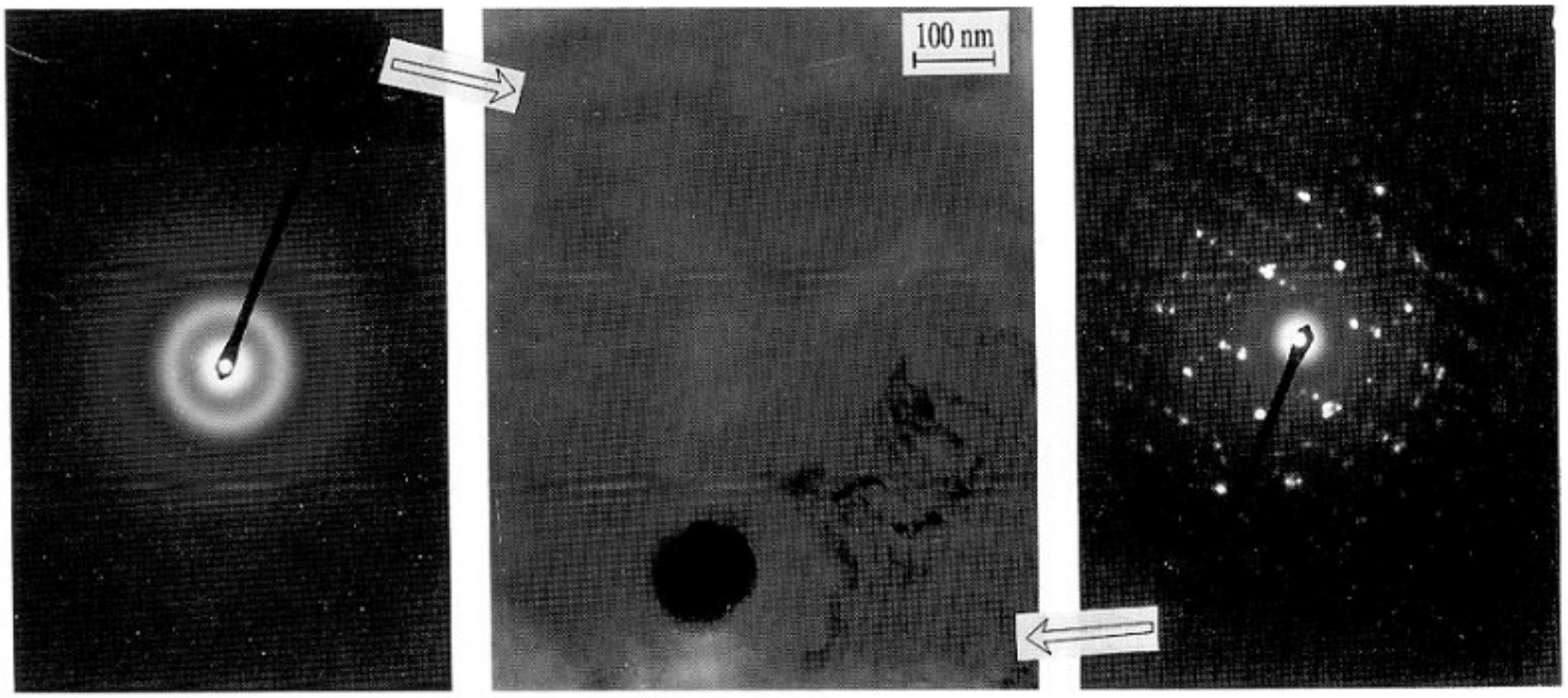

Fig. 7. Detail from the Nb filament depicted in Fig. 6 (rolled and annealed). The crystalline phase growths into the glassy area ($T=873$ K, $t\approx 120$ s).

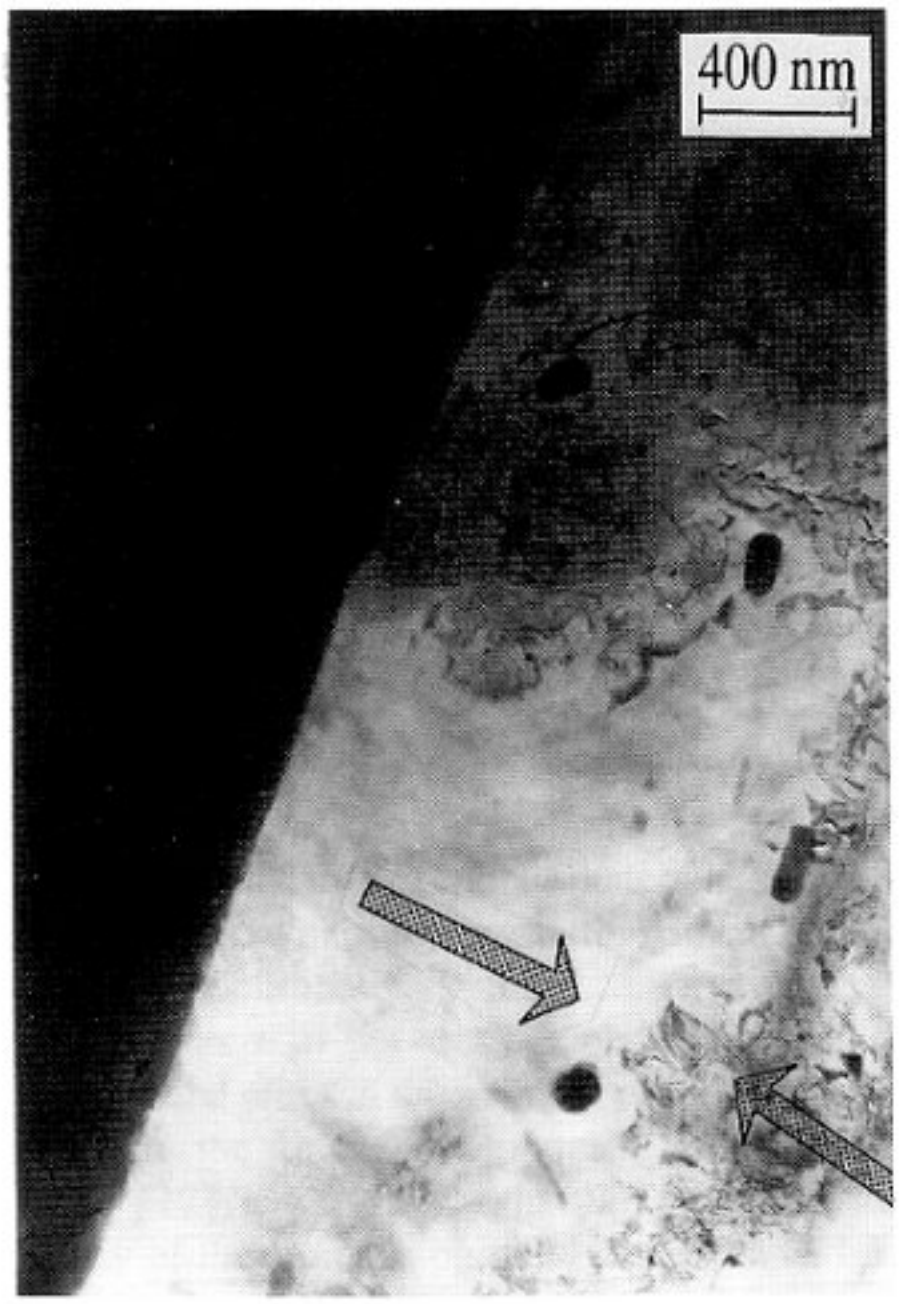

Fig. 6. Annealed Nb filament containing a non-crystalline area ($\epsilon=99.4\% + T=873$ K, $t\approx 60$ s). Begin of crystallization by movement of glass–crystal phase boundaries. Detail marked by arrow.

i.e. the crystalline filament width is decreased by 50%, for typical values of t the critical stress increases hence by a factor of about 1.8.

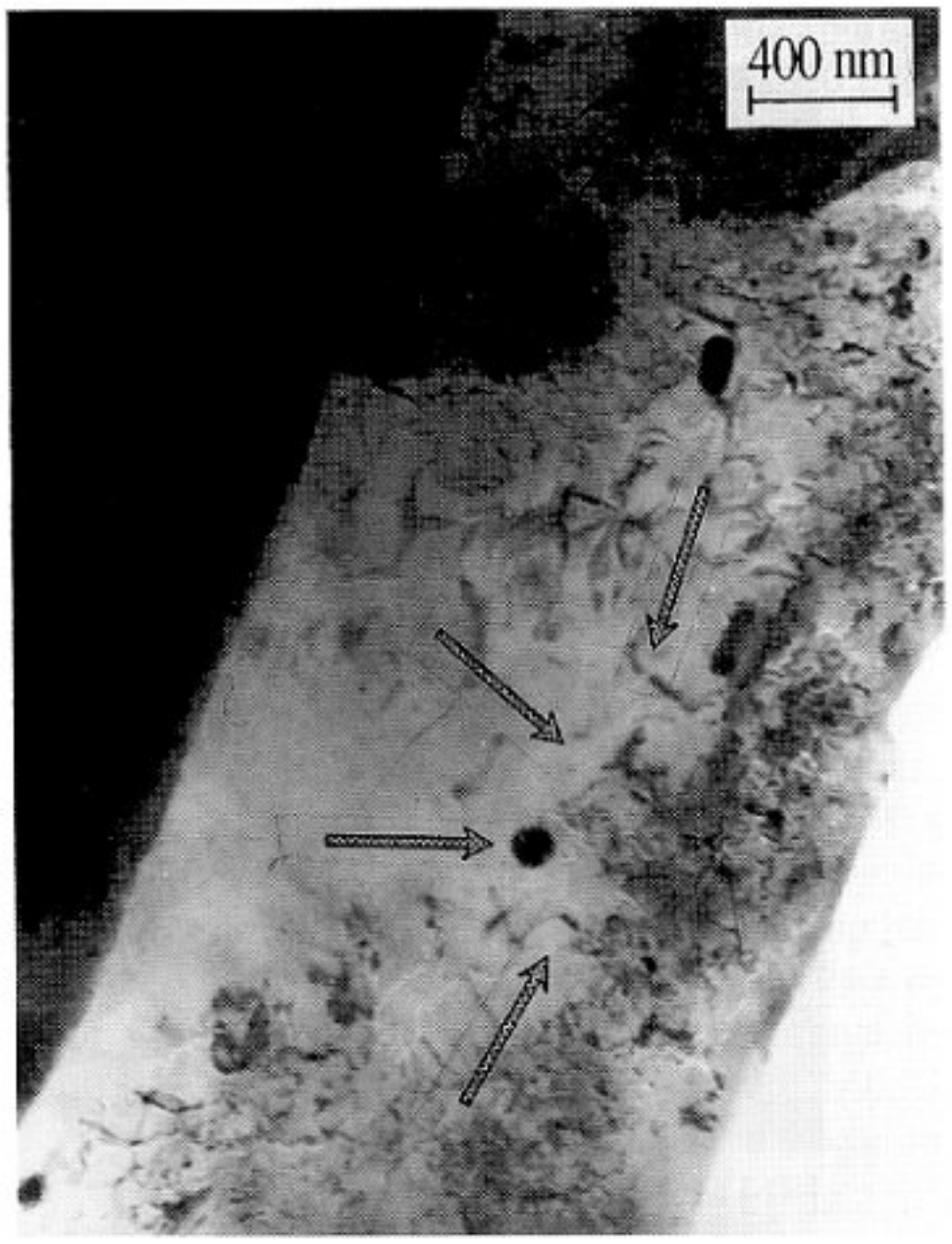

Fig. 8. Flat section of the Nb filament shown in Fig. 6. Partial crystallization by movement of glass–crystal phase boundaries after an additional heat treatment at 973 K for 2 min and subsequent quenching to 923 K ($\epsilon=99.4\%$). The area already shown in detail in Fig. 7, reveals further shrinkage of the glassy phase (arrows).

4. Conclusions

A Cu–20 wt% Nb in situ composite was heavily cold rolled. Nb filaments were extracted and investigated by use of TEM, SAD, EDX and HRTEM (flat sections). In the filaments elongated dislocation cells as well as randomly arranged dislocation networks were observed. The main result, however, was the discovery of numerous non-crystalline areas, which in part extended over the entire filament widths. The shrinkage, i.e. crystallization of glassy areas during annealing was directly observed in the TEM.

References

[1] D.J. Chakrabati and D.E. Laughlin, Bull. Alloy Phase Diagramms 2 (1982) 936.
[2] G.I. Terekhov and L.N. Aleksandrova, Izv. Akad. Nauk SSR. Metall. 4 (1984) 210.
[3] C. Trybus and W.A. Spitzig, Acta Metall. 37 (1989) 1971.
[4] D. Raabe, J. Ball, and G. Gottstein, Scr. Metall. 27 (1992) 211.
[5] D. Raabe and G. Gottstein, J. Phys. (Paris) IV, Col. C7, Sup. J. Phys. (Paris) III 3 (1993) 1727.
[6] J. Bevk, J.P. Harbison and J.L. Bell, J. Appl. Phys. 49 (1978) 6031.
[7] W.A. Spitzig, A.R. Pelton and F.C. Laabs, Acta Met. Mater. 35 (1987) 2427.
[8] W.A. Spitzig and P. Krotz, Scr. Met. Mater. 2 (1987) 1143.
[9] D. Raabe and F. Heringhaus, Phys. Stat. Sol. 142a (1994) 473.
[10] J. Bevk and K.R. Karasek, in: New Development and Applications in Composites., eds. D. Kuhlmann-Wilsdorf and W.C. Harrigan (AIME, Warrendale, PA, 1979) p. 101.
[11] K.R. Karasek and J. Bevk, J. Appl. Phys. 52 (1981) 1370.
[12] A.R. Pelton, F.C. Laabs, W.A. Spitzig and C.C. Cheng, Ultramicroscopy 22 (1987) 251.
[13] A.S. Argon, Mater. Sci. Tech. 6 (1993) 461.
[14] F. Heringhaus, D. Raabe, L. Kaul and G. Gottstein, Metall. 6 (1993) 558.
[15] F. Heringhaus, D. Raabe and G. Gottstein, Metall. 48 (1994) 287.
[16] F. Heringhaus, D. Raabe, U. Hangen and G. Gottstein, Mater. Sci. Forum 157–162 (1994) 709.
[17] D. Raabe and U. Hangen, in press.
[18] J.G. Sevillano, J. Phys. (Paris) III 6 (1990) 967.